Stochastic Analysis of Single-Hop Communication Link in Vehicular Ad Hoc Networks

Khadige Abboud, *Student Member, IEEE,* and Weihua Zhuang, *Fellow, IEEE*

Abstract—A vehicular ad hoc network (VANET) is a promising addition to our future intelligent transportation systems, which supports various safety and infotainment applications. The high node mobility and frequent topology changes in VANETs impose new challenges on maintaining a long-lasting connection between network nodes. As a result, the lifetime of communication links is a crucial issue in VANET development and operation. This paper presents a probabilistic analysis of the communication link in VANETs for three vehicle density ranges. Firstly, we present the stationary distribution of the communication link length using mesoscopic mobility models. Secondly, we propose a stochastic microscopic mobility model that captures time variations of inter-vehicle distances (distance headways). A discrete-time finite-state Markov chain with state dependent transition probabilities is proposed to model the distance headway. Thirdly, the proposed stochastic microscopic model and first passage time analysis are used to derive the probability distribution of the communication link lifetime. Numerical results are presented to evaluate the proposed model, which demonstrate a close agreement between analytical and simulation results.

Keywords—*Vehicle mobility, communication link, microscopic mobility, mesoscopic mobility, vehicle traffic flow.*

I. Introduction

IN recent years, there have been extensive R&D activities to develop vehicular ad hoc networks (VANETs) on the transport infrastructure, which will enable communications among vehicles and road-side units [2]. VANETs are expected to enhance the intelligent transportation systems (ITS) and support not only public-safety applications, but also a wide range of infotainment applications.

Unlike traditional mobile ad hoc networks, the high node mobility in VANETs can cause frequent network topology changes and fragmentations. Moreover, VANETs are susceptible to vehicle density variations from time to time throughout the day. This imposes new challenges in maintaining a connection between vehicular nodes. The length of the communication link and its lifetime between network nodes are critical issues that determine the performance of network protocols. From a routing protocol perspective, the communication link length, i.e., the hop length, determines the route length between source and destination pairs. The route length is an important metric in shortest path algorithms, which are a base of many routing protocols. Additionally, a short communication link lifetime can disrupt an ongoing packet transmission between two nodes, thus triggering a new route discovery procedure. The interruptions of information transmissions not only lead to a reception failure, but can also result in wastage of the limited radio bandwidth. From a medium access control (MAC) perspective, the communication link length determines the amount of channel spatial reuse and the amount of channel access that the nodes within a hop have. Simulations of the IEEE 802.11p standard MAC protocol have shown that a large relative speed between nodes (i.e., short link lifetime) reduces the

K. Abboud and W. Zhuang are with the Center for Wireless Communications, Department of Electrical and Computer Engineering, University of Waterloo, 200 University Avenue West, Waterloo, Ontario, Canada, N2L 3G1. E-mail: {khabboud,wzhuang}@uwaterloo.ca

channel access time of vehicular nodes [3]. Furthermore, the diverse potential applications for VANETs vary in their connection time requirements. For example, safety applications do no require a long link lifetime when compared to multimedia applications [2]. Hence, analyzing the communication link length and lifetime is essential for designing efficient routing and MAC protocols that support different application requirements in VANETs [3], [4].

A distance headway is the distance between identical points on two consecutive vehicles on the same lane. The distance headway and its variations over time play an essential role in determining both the communication link length and its lifetime. Modeling vehicle traffic characteristics (e.g., the headways) has attracted great attention from researchers in transportation engineering for many years. In general, vehicle mobility models in the literature can be categorized into three (microscopic, mesoscopic, and macroscopic) types according to the detail level of the interactions among vehicles that the model characterizes [5]–[7]. A macroscopic distance headway model describes the average distance headway over a highway. On a mesoscopic level, the distance headways of individual vehicles are described by independent and identically distributed random variables [5], [8]. A microscopic model specifies time variations of a distance headway according to the driver behaviors and interactions with neighboring vehicles [5], [6]. Mesoscopic models are used to model the communication link length between two network nodes [8]. Given an available communication link with a certain length, the knowledge of the link duration (lifetime) is of major importance especially for applications with high rate contents and strict delay requirements. In the literature, there are studies to model the communication link lifetime based on mesoscopic models and/or deterministic microscopic properties (e.g., [8]). However, the two main factors that affect changes of a distance headway over time, i.e., the driver behaviors and interactions with neighboring vehicles, are both random. Furthermore, the correlation between a distance headway and its changes over a time period is not captured in a mesoscopic model. Therefore, to accurately model the communication link lifetime, a microscopic mobility model should be used. In general, microscopic mobility models in the literature include a set of deterministic and/or probabilistic rules that define how a vehicle on road changes its speed and/or acceleration in reaction to its neighboring vehicles' behaviors [5]. As such a model depends on the behaviors of neighboring vehicles over time, the analysis tends to take the form of case studies (e.g., [8]).

In this paper, we present a stochastic analysis of the communication link, based on the three types of distance headway models. On a macroscopic level, we consider three levels of average distance headways, corresponding to different traffic flow conditions. For each traffic flow condition, we employ the associated mesoscopic distance headway model to derive the probability distribution of the communication link length. We propose a microscopic model that describes the time variations of a distance headway. The model takes into account the dependency of the changes of a distance headway on its current value. We validate the proposed dependency using empirical and simulated highway data. With the proposed stochastic microscopic model, we derive the probability distribution of the communication link lifetime using the first passage time analysis. Finally, we simulate
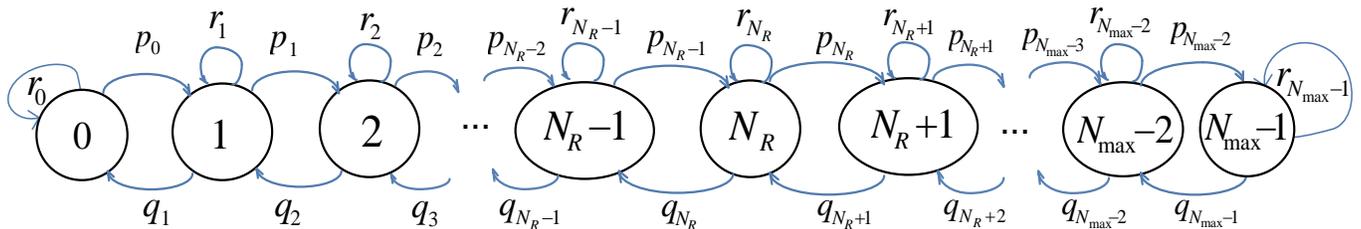
Figure 1. An illustration of the proposed discrete-time $N_{\max}$-state Markov chain model of the distance headway

highway vehicular traffic using microscopic vehicle traffic simulator, VISSIM, and demonstrate that the analytical results of our model match well with simulation results.

II. SYSTEM MODEL

Consider a VANET on a multi-lane highway with no on or off ramps. We focus on vehicles in a single lane with lane changes implicitly captured in our analysis. We choose to model a single lane from a multi-lane highway instead of a single-lane highway, in order to be more realistic in a highway scenario. A vehicle can overtake a slower leading vehicle, if possible, and accelerate towards its desired speed[1]. Assume that the highway is in a steady traffic flow condition defined by a time-invariant vehicle density, and denote the vehicle density on the lane under consideration by D in vehicles per kilometer (veh/km). Let μ and σ be the mean and the standard deviation of the distance headway in meters, respectively, where $\mu = 1000/D$ and σ are constant system parameters and take different values according to the vehicle density. Time is partitioned with a constant step size τ. Let $X_i = \{X_i(m), m = 0, 1, 2, \ldots\}$ be a discrete-time stochastic process of the ith distance headway, between node i and node $i + 1$, where $X_i(m)$ is a random variable representing the distance headway of node i at the mth time step, $i = 0, 1, 2, \ldots$, $m = 0, 1, 2, \ldots$. For notation simplicity, we omit the index i when referring to an arbitrary distance headway. At any time step, $X_i(m) \in [\alpha, X_{\max}]$ for all $i, m \geq 0$, where α and $X_{\max}$ is the minimum and maximum inter-vehicle distances, respectively. Furthermore, assume that X_i's are independent with identical statistical behaviors for all $i \geq 0$. All the vehicles have the same transmission range, denoted by R. Any two nodes at a distance less than R from each other are one hop neighbors. Assume that the transmission range is much larger than the width of the highway such that a node can communicate with any node within a longitudinal distance of less than R from it. The length of a hop is defined as the distance to the furthest node within the transmission range of a reference node, which is upper bounded by R.

Table I. Traffic flow condition for different vehicle densities [5]

Density (veh/km)	Traffic flow condition	
0 − 7	Free-flow operations	Uncongested flow conditions (low density)
7 − 12	Reasonable free-flow operations	
12 − 19	Stable operations	
19 − 26	Borders on unstable operations	
26 − 42	Extremely unstable flow operations	Near-capacity flow conditions (intermediate density)
42 − 62	Forced of breakdown operations	Congested flow conditions (high density)
> 62	Incident situation operations	

III. VEHICLE MOBILITY MODEL

To characterize how the distance headway and its variations over time affect the communication link lifetime, we characterize the distance headway based on vehicular mobility models. On a macroscopic level, we consider three different traffic flow conditions: uncongested, near-capacity, and congested. In this work, we study each of the three traffic flow conditions separately, without considering the case of changing traffic flow condition. Each traffic flow condition corresponds to a range of vehicle densities according to Table I [5]. The uncongested, near capacity, and congested traffic flow conditions correspond to low, intermediate, and high vehicle densities, respectively. Additionally, each traffic flow condition corresponds to a unique microscopic and a unique mesoscopic distance headway model.

A. Mesoscopic mobility model

Main mesoscopic models in the literature focus on the time-headway, which is the elapsed time of the passage of identical points on two consecutive vehicles [5]. For an uncongested traffic flow condition, the exponential distribution has been shown to be a good approximation for the time headway distribution [5]. With a low vehicle density, interactions between vehicles are very low and almost negligible. As a result, vehicles move independently at a maximum speed [5]. It is reasonable to assume that, over a short time interval of interest, vehicles move at constant velocity and do not interact with each other [10], [11]. Therefore, for a low vehicle density, we assume that the distance headway has the same distribution as the time headway with parameters properly scaled. The inter-vehicle distances X_i's at any time step are independent and identically distributed (i.i.d.) with an exponential probability density function (pdf)

$$f_{X_i}(x) = \frac{1}{\mu}e^{-\frac{x}{\mu}}, \quad x \geq 0. \tag{1}$$

In this case, the mean and the standard deviation of the distance headway is $\mu = \sigma = \frac{1000}{D}$. According to the distribution, $P(X_i \leq \alpha) > 0$; however, for simplicity, we ignore the effect of this probability[2].

In the literature, the Gaussian distribution is used to model the time headway for a congested traffic flow condition [5]. Although the time headway is almost constant for a high vehicle density, driver behaviors cause the time headway to vary around that constant value. Therefore, the Gaussian distribution model for the time headway characterizes the driver attempt to drive at a constant time headway [5]. With the same argument, we assume that the distance headways vary around a constant value with a Gaussian distribution. The pdf of the distance headway is

---

[1]In a single-lane highway, the vehicle traffic gradually converges into a number of platoons lead by the slower vehicles on the highway [9].

[2]$P(X_i \leq \alpha) = 1 - e^{-D\alpha}$. For example, for $D = 6$ veh/km and $\alpha = 6.7$ meters [5], $P(X_i \leq \alpha) = 0.04$. The probability $P(X_i \leq \alpha)$ increases with D.

approximately given by

$$f_{X_i}(x) = \frac{1}{\sqrt{2\pi}\sigma} e^{-\frac{(x-\mu)^2}{2\sigma^2}}, \quad x \geq 0. \tag{2}$$

The standard deviation σ for a high vehicle density is given by[3] $\sigma = \frac{(\mu - \alpha)}{2}$.

For a near-capacity traffic flow condition, empirical pdfs for inter-vehicle distances show that neither an exponential nor a Gaussian distribution is a good fit [12]. Hence, we assume that the inter-vehicle distances follow a general distribution, Pearson type III, that was originally proposed for time headways [5]. With an intermediate vehicle density, the pdf of the distance headway is approximately given by

$$f_{X_i}(x) = \frac{\lambda^z}{\Gamma(z)}(x-\alpha)^{z-1}e^{-\lambda(x-\alpha)}, \quad x \geq \alpha \tag{3}$$

where λ and z are the scale and shape parameters of the general Pearson type III distribution, respectively, and $\Gamma(z) = \int_0^\infty u^{z-1}e^{-u}du$ is the gamma function. The parameters λ and z are related to μ and σ according to the following relations [5]

$$\lambda = \frac{\mu - \alpha}{\sigma^2}, \quad z = \frac{(\mu - \alpha)^2}{\sigma^2}. \tag{4}$$

B. Microscopic mobility model

We model the stochastic process, X_i, as a discrete-time finite-state Markov chain, inspired by [12], [13]. The Markov chain, illustrated in Figure 1, has $N_{\max}$ states corresponding to $N_{\max}$ ranges of a distance headway. The length of the range covered by each state is a constant, denoted by L in meters. The jth state covers the range $[x_j, x_j + L)$, $0 \leq j \leq N_{\max} - 1$, where $x_j = \alpha + jL$. At any time step, $X_i(m) = x_j$ denotes that the distance headway X_i is in the jth state, for all $i, m \geq 0$, and $0 \leq j \leq N_{\max} - 1$. Let $N_R = \frac{R - \alpha}{L}$ be the integer number of states that cover distance headways within R. Hence, the states with indices $j \in \{0, 1, 2, \ldots, N_R - 1, N_R, N_R + 1, \ldots, N_{\max} - 2,$ and $N_{\max} - 1\}$ correspond to the quantized distances $x_j \in \{\alpha, \alpha + \frac{R-\alpha}{N_R}, \alpha + 2\frac{R-\alpha}{N_R}, \alpha + 3\frac{R-\alpha}{N_R}, \ldots, \alpha + \frac{R-\alpha}{N_R/(N_R-1)}, R, \alpha + \frac{R-\alpha}{N_R/(N_R+1)}, \ldots, X_{\max} - \frac{R-\alpha}{N_R}, \text{ and } X_{\max}\}$, respectively. Within a time step, a distance headway in state j can transit to the next state, the previous state, or remain in the same state with probabilities p_j, q_j, or r_j, $0 \leq j \leq N_{\max} - 1$, respectively. Without loss of generality, assume that probability transition matrix is a positive-definite tri-diagonal and is given by

$$M = \begin{pmatrix} r_0 & p_0 & 0 & \cdots & & \cdots & 0 \\ q_1 & r_1 & p_1 & 0 & & \cdots & \vdots \\ 0 & q_2 & r_2 & p_2 & 0 & & \vdots \\ \vdots & \ddots & \ddots & \ddots & & \ddots & 0 \\ 0 & \cdots & 0 & q_{N_{\max}-2} & r_{N_{\max}-2} & p_{N_{\max}-2} \\ 0 & \cdots & \cdots & 0 & q_{N_{\max}-1} & r_{N_{\max}-1} \end{pmatrix}. \tag{5}$$

The tri-diagonal structure of M is due to the fact that the values of a distance headway at consecutive time steps are highly correlated, for a short time step, such as $\tau \leq \frac{L}{\bar{v}}$, where $\bar{v}$ is the maximum relative speed between vehicles[4]. We propose to use the following state-dependent transition probability functions

---

[3]We use the same guidelines for calculating the variance of time headway as given in [5]. With $\sigma = \frac{(\mu-\alpha)}{2}$, $P(X_i > \alpha) = 0.977$ [5]. For a congested traffic flow condition (i.e., $D \geq 42$ veh/km) and $\alpha = 6.7m$ [5], $P(X_i \leq 0) \leq 2.8 \times 10^{-3}$.

[4]Consider an i.i.d. desired vehicle speed with a mean of 100 kilometer per hour and a standard deviation of 10 kilometer per hour, i.e., $P(\bar{v} \leq 36) = 0.99$. In this case, the choice of $\tau = 2$ seconds for $L = 20$ meters, reduces the transition probability of the distance headway to a non-neighboring state to less than 0.0054
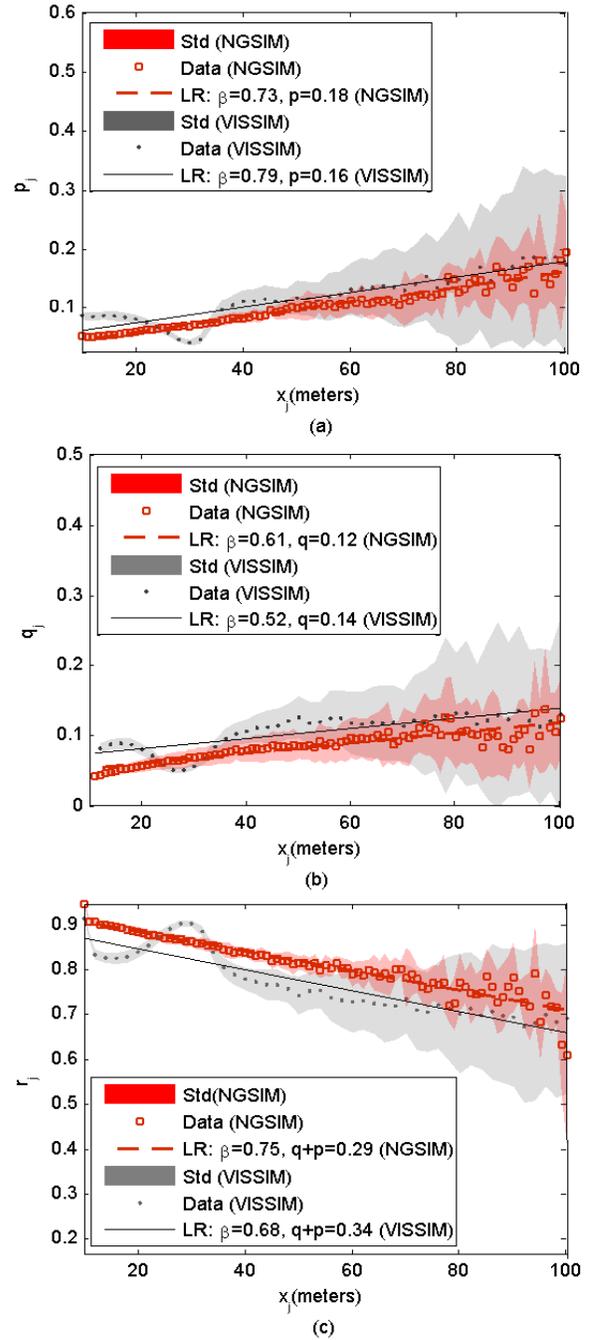

Figure 2. The transition probability from state j to (a) state $j+1$, (b) state $j-1$, and (c) state j, for different x_j values from NGSIM and VISSIM data for intermediate to high vehicle densities. Results for the weighted linear regression (LR) fit model for (6) are given in the legends.

$$\begin{aligned} p_j &= p\left(1 - \beta\left(1 - \frac{x_j}{X_{\max}}\right)\right) \\ q_j &= q\left(1 - \beta\left(1 - \frac{x_j}{X_{\max}}\right)\right) \\ r_j &= 1 - p_j - q_j, \ 0 \leq j \leq N_{\max} - 1, \ 0 \leq p, q, \beta \leq 1 \end{aligned} \tag{6}$$

where p, q, and β are constants that depend on the vehicle density. For a low vehicle density, β is close to zero, and therefore the transition probabilities are independent of the state value, x_j. The value of β increases as the vehicle density increases, and thus increases the dependency on the state value. Eq.(6) can be explained as follows. In a low vehicle density, distance headways
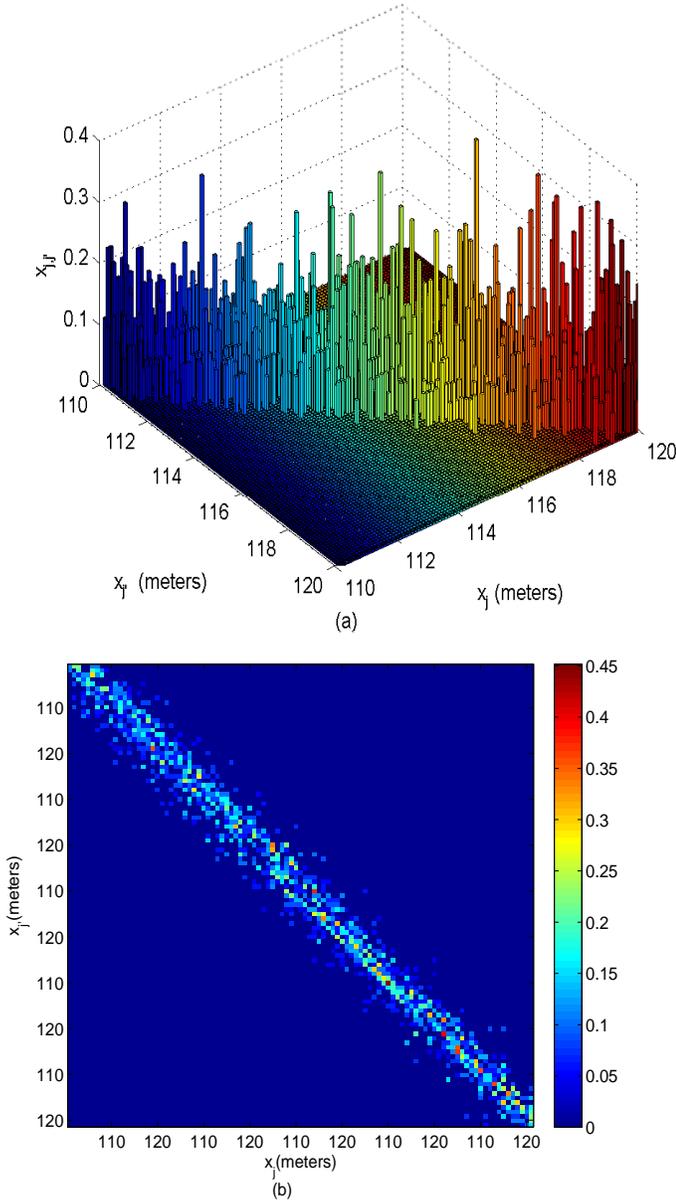
tion probability matrix using i) empirical vehicle trajectory data collected from highways provided by Next Generation Simulation (NGSIM) online database [14], and ii) simulated vehicle trajectory data generated by VISSIM microscopic vehicle traffic simulator. The vehicles in VISSIM simulator move according to Wiedemann's microscopic mobility model. Wiedemann is psycho-physical car-following model that describes behaviors of individual vehicles according to their interactions with neighboring vehicles, their desired relative speeds, their relative positions, and some driver-dependant behaviors. The Wiedemann model accounts for four different driving modes: free driving, approaching, following, and breaking [15]. We adopt the Wiedemann 99 model which is designed for a highway scenario with its parameters set to the default values suggested in [16]. We use two NGSIM data sets: *I-80-Main-Data* and *US-101-Main-Data*, which were collected from a seven lane highway for a section of 500 and 640 meters, respectively. From the NGSIM data sets, we exclude data points associated with vehicles 1) on an on-ramp lane, 2) on an off-ramp lane, 3) at the end of the section, or 4) undertaking a lane change. The VISSIM data set was obtained via six 30-minute simulations of a three-lane highway traffic for different vehicle densities. The highway is a closed loop, and the vehicles enter the highway with a traffic flow of (3052.8, 1914.2, 854.6, 683.7, and 379.8) vehicle per hour per lane for 1000 seconds, resulting in vehicle densities of (42, 26, 16, 9, and 5), respectively. The VISSIM data points associated with vehicles entering the highway or changing lanes are not included in our analysis. To obtain the transition probabilities, the NGSIM and VISSIM data sets are mapped into a sequence of quantized state values (x_j) with a predefined state length L, where $x_j \in [0, X_{\max}]$ in meters and $0 \le j \le N_{\max} - 1$. The NGSIM data is only available with intermediate-to-high vehicle densities with $X_{\max} = 100$ meters. For each state j, the transition probabilities for the distance headway are determined by counting the number of occurrences of each transition. Let $n_{j,j'}$ be the number of transitions of a distance headway from state j to state $j', 0 \le j' \le N_{\max} - 1$, within a time step of length τ, and $n_j = \sum_{j'=0}^{N_{\max}-1} n_{j,j'}$ be the number of time steps at which the distance headway is in state j. The transition probability from state j to j' is calculated by $p_{j,j'} = \frac{n_{j,j'}}{n_j}, \quad 0 \le j, j' \le N_{\max} - 1$.

Figure 2 plots the transition probabilities (and their standard deviation) from state j to its direct neighboring states and to itself for different x_j values, with the default data recording values: $L = 1$ meter and $\tau = 0.1$ seconds for the NGSIM data set, and $L = 2$ meters and $\tau = 0.2$ seconds for the VISSIM data set. The results show a dependency of the transition probabilities on the x_j value. The weighted linear regression (LR) is used to fit the transition probabilities in Figure 2, with $n_{j,j'}$ being the weight of each $p_{j,j'}$ data point. The transition probabilities p_j and q_j increase with the quantized state value, x_j, which agrees with (6). The values of p, q, and β are calculated according to the resulting weighted linear regression (LR) fit and are given in the figure legends. The results show that $p_{j,j'}$ is smaller than 10^{-3} for $|j - j'| > 1$, and is therefore neglected, which is consistent with the tri-diagonal transition matrix assumption given in (5). Figure 3 plots the transition probability matrix calculated from the NGSIM data for $x_j, x_{j'} \in [110, 120]$, $L = 0.1$ meters, and $\tau = 0.1$ seconds. It is observed from Figure 3 that, for a reduced value of the ratio L/τ, $p_{j,j'}$ increases for $|j - j'| > 1$. Figure 4 plots the transition probability to the next state (and its standard deviation) for different x_j values and different vehicle densities. The results show that, the larger the vehicle densities, the higher the state-dependency of the transition probabilities. The resulting β values for different vehicle densities are plotted in Figure 5, which shows an approximate linear relation between β and the vehicle density.

Figure 3. **Probability transition matrix for 100 quantized values of $x_j, x_{j'} \in [110, 120]$ with $L = 0.1$ meters and $\tau = 0.1$ seconds. The matrix is calculated based on NGSIM data.**

are relatively large. Hence, a vehicle moves freely with a desired speed [5]. In such a scenario, the distance headway value does not affect the driver's choice to keep/change the speed, since the distance headway is large enough. On the other hand, in a high vehicle density situation, distance headways are relatively small. Hence, vehicles move with high constraints to keep a safe distance ahead. In such a scenario, the distance headway value has a high impact on the driver's behavior and his/her choice to keep/change the speed (and consequently the distance headway). The constant β is comparable with the driver strain constant used in [6], whereas $\beta = 0$ in [7]. The transition probabilities of the distance headway to neighboring states increase with the distance headway value, when $\beta > 0$ in (6). This is due to the fact that a larger distance headway results in less constraints in driving.

In order to verify the dependency of the distance headway transition probability on its current state, we compute the transi-
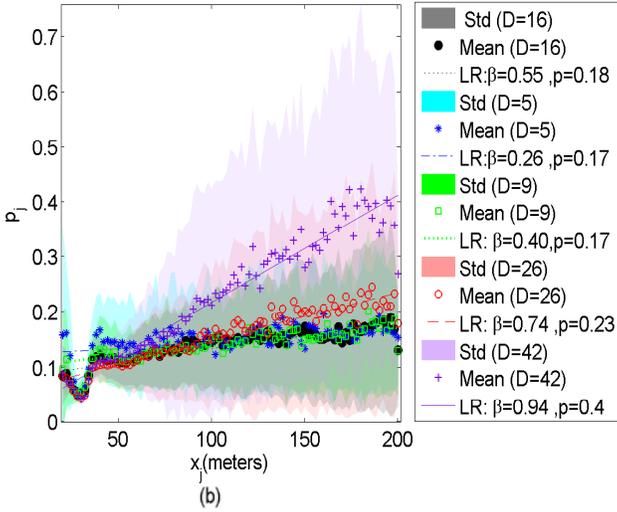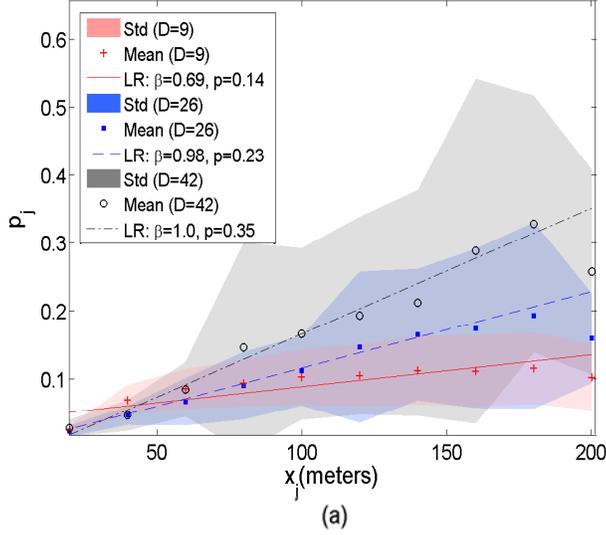
(a)

(b)

Figure 4. Transition probability from state j to state $j+1$, for different x_j values from VISSIM data for vehicle densities of (a) 9, 26, and 42 veh/km with $L = 20$ meters and $\tau = 2$ seconds and (b) 5, 9, 16, 26, and 42 veh/km, with $L = 2$ meters and $\tau = 0.2$ seconds. Results of the weighted linear regression fit model for (6) are given in the legends.

Figure 5. State dependency parameter, β for different D values calculated based on VISSIM data.

This agrees with our proposed transition probability functions in (6).

It should be noted that the proposed microscopic model does not explicitly describe how and when lane changes occur nor does it describe impacts of lane-changes on the time variations of distance headways. However, the model implicitly captures the impact of lane changes on maintaining the ability of the vehicles to overtake slower vehicles and accelerate towards their desired speed. This is captured in the parameters $p, q,$ and β which can be tuned from empirical/simulated multi-lane highway trajectory data for one of the lanes as done earlier in this section.

IV. DISTRIBUTION OF THE COMMUNICATION LINK LENGTH

In this section, we present the probability distribution of the communication link length using mesoscopic distance headway models. The hop length (or the link length), denoted by H, is the distance from a reference node to the furthest node within the transmission range of the reference node, which is upper bounded
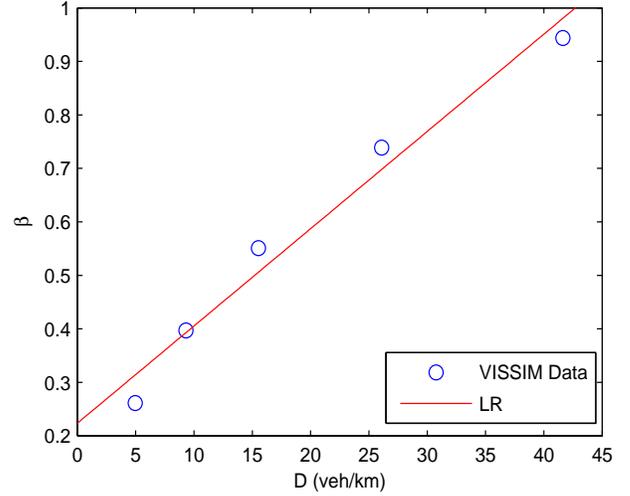
by the transmission range R. Given a mesoscopic model, the distance headways X_i's are i.i.d. with probability density function $f_X(x)$ and cumulative distribution function (cdf) $F_X(x)$. Let $Q(l)$ be the event that there exists at least one node within distance l from a reference node. The event $Q(l)$ occurs with probability $F_X(l)$. Let $Q^c(l)$ be the complement of event $Q(l)$, i.e., the event that there are no nodes within distance l from a reference node. Then, the cdf of H is given by [17]

$$F_H(h) = \frac{P(Q^c(R-h), Q(h))}{P(Q(R))}. \quad (7)$$

The pdf can then be calculated by $f_H(h) = \frac{d}{dh_r} F_H(h)$. For a low vehicle density, the distance headway is exponentially distributed with pdf given in (1). The pdf of the corresponding hop length is given by [18]

$$f_H(h) = \frac{e^{-\frac{(R-h)}{\mu}}}{\mu(1 - e^{-\frac{R}{\mu}})}, \quad 0 < h < R \quad (8)$$

which is a scaled exponential distribution truncated at R. For an intermediate vehicle density, the distance headways are i.i.d., each following the Pearson type III pdf in (3). The cdf for the first hop length can be derived from (7) and the corresponding pdf is found to be

$$
\begin{aligned}
f_H(h) &= \frac{1}{\gamma(z, \lambda(R - \alpha))}[f_X(R - h)\gamma(z, \lambda(h - \alpha) \\
&\quad + f_X(h)\Gamma(z, \lambda(R - h - \alpha))], \alpha \le h < R - \alpha
\end{aligned}
\quad (9)
$$

where $\gamma(z, x) = \int_0^x t^{z-1} e^{-t} dt$ and $\Gamma(z, x) = \int_x^\infty t^{z-1} e^{-t} dt$ are the lower and the upper incomplete gamma functions, respectively, and $f_X(\cdot)$ is given by (3). The derivation for $f_H(h)$ is given in Appendix A.

For a high vehicle density, the distance headways are i.i.d., each following the Gaussian pdf in (2). Using the cdf of the Gaussian distribution, $F_X(x) = \frac{1}{2}\left(1 + \text{erf}\left(\frac{x-\mu}{\sqrt{2}\sigma}\right)\right)$, the cdf for

the hop length can be derived from (7) and is given by

$$
\begin{aligned}
f_H(h) = {} & \frac{1}{\sqrt{2\pi}\sigma}\left(1 + \mathrm{erf}\left(\frac{R-\mu}{\sqrt{2}\sigma}\right)\right)^{-1} \times \left[e^{-\frac{(h-\mu)^2}{2\sigma^2}} \right. \\
& \times \left(1 - \mathrm{erf}\left(\frac{R-h-\mu}{\sqrt{2}\sigma}\right)\right) + e^{-\frac{(R-h-\mu)^2}{2\sigma^2}} \\
& \times \left. \left(1 + \mathrm{erf}\left(\frac{h-\mu}{\sqrt{2}\sigma}\right)\right)\right], \quad 0 < h < R \quad (10)
\end{aligned}
$$

where $\mathrm{erf}(\cdot)$ is the error function, given by $\mathrm{erf}(x) = \frac{2}{\sqrt{\pi}}\int_0^x e^{-t^2}dt$.

V. COMMUNICATION LINK LIFETIME

Consider a communication hop from an arbitrary reference node in the direction of the vehicle traffic flow. The reference node is one hop away from all the nodes within a distance less than R (assuming that an on/off link depends only on the distance between the nodes). Define the communication link lifetime between two nodes as the first time step at which the distance between the two nodes is larger than or equal to R, given that the distance between them is less than R at the 0th time step. For any node within R from the reference node, the communication link lifetime is at least equal to the that of the furthest node from the reference vehicle (referred to as *hop edge node*). A study of the communication link lifetime of the edge vehicle from its reference vehicle is presented in the following.

A. First passage time between two distance headway states

Let $T_{j,j'}^i$, $0 \le j, j' \le N_{\max} - 1$, be the first passage time of the distance headway X_i to state j' given that the distance headway is in state j at the 0th time step, i.e., $T_{j,j'}^i = inf\{m > 0; X_i(m) = x_{j'}, X_i(0) = x_j\}, 0 \le j \le N_{\max} - 1$ ($inf\{\cdot\}$ is the Infimum). In the following, $T_{j,j'}$ is used without superscript i for an arbitrary distance headway. Let M' be an $N_{\max} \times N_{\max}$ matrix equal to M with $q_{N_{\max}-1} = 0$ and $r_{N_{\max}-1} = 1$. Let $\{\lambda_u\}_{u=0}^{N_{\max}-2}$ be the $N_{\max} - 1$ non-unit eigenvalues of M'. The first passage time to state $N_{\max} - 1$, given that $X_i(0) = x_0$, is the sum of $N_{\max} - 1$ independent geometric random variables, each with a mean equal to $\frac{1}{1-\lambda_u}$ [19]. The probability generating function of $T_{0,N_{\max}-1}$ is given by

$$
G_{T_{0,N_{\max}-1}}(v) = \prod_{u=0}^{N_{\max}-2}\left[\frac{(1-\lambda_u)v}{1-\lambda_u v}\right]. \quad (11)
$$

The probability mass function (pmf) of $T_{0,N_{\max}-1}$ is then calculated by $P_{T_{0,N_{\max}-1}}(m) = \frac{G_{T_{0,N_{\max}-1}}^{(m)}(0)}{m!}$, where $G_{T_{0,N_{\max}-1}}^{(m)}(0)$ is the value of the mth derivative of $G_{T_{0,N_{\max}-1}}(v)$ at $v = 0$.

Let $M^{(j)}$ be a $(j+1) \times (j+1)$ matrix, $0 < j < N_{\max} - 1$, equal to the upper left $(j+1) \times (j+1)$ portion of matrix M with $q_j = 0$ and $r_j = 1$. The first passage time of the distance headway to state j, given that the initial distance headway is in state 0, has a probability generating function $G_{T_{0,j}}(v) = \prod_{u=0}^{j-1}\left[\frac{(1-\lambda_u^{(j)})v}{1-\lambda_u^{(j)}v}\right]$, where $\lambda_u^{(j)}$, $u = 0, 1, \ldots, j-1$, are the j non-unit eigenvalues of $M^{(j)}$. Note that the distance headway cannot move to state $j'(> j)$ before passing through state j in a birth and death process. Using $T_{0,j'} = T_{0,j} + T_{j,j'}$, the passage time to state j' given that the initial distance headway is in state j, $0 \le j < j' \le N_{\max} - 1$, can be calculated. The probability generating function of $T_{j,j'}$ is $G_{T_{j,j'}}(v) = \frac{E\left[v^{T_{0,j'}}\right]}{E\left[v^{T_{0,j}}\right]}$,
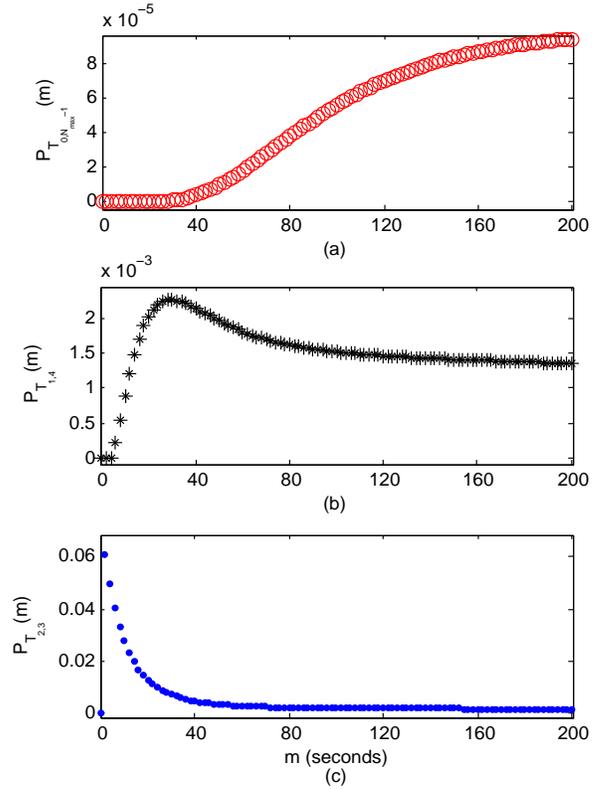
Figure 6. **Probability mass function of the first passage time for (a) $T_{1,N_{\max}}$, (b) $T_{1,4}$, and (c) $T_{2,3}$, with mean values of 19.8×10^3, 1.24×10^3, and 318.4 seconds, respectively, with parameters $N_{\max} = 9, L = 20$ meters, $\tau = 2$ seconds, $X_{\max} = 160$ meters, $\beta = 0.66, p = 0.12$, and $q = 0.26$.**

and is calculated by

$$
G_{T_{j,j'}}(v) = v^{j'-j}\frac{\prod_{u=0}^{j'-1}\left[\frac{(1-\lambda_u^{(j')})}{1-\lambda_u^{(j')}v}\right]}{\prod_{u=0}^{j-1}\left[\frac{(1-\lambda_u^{(j)})}{1-\lambda_u^{(j)}v}\right]}. \quad (12)
$$

Figure 6 plots the pmf's of $T_{0,N_{\max}-1}$, $T_{1,4}$ and $T_{2,3}$ for a nine-state distance headway model. The pmf's are evaluated using MAPLE [20]. Figure 6 shows that the probability of the first passage time, $T_{j,j'}$, taking on a small value decreases as the number of states, $|j'-j|$, increases.

B. First passage time of the sum of distance headways

The distance between a reference node and its hop edge node is equal to the sum of the distance headways between the two nodes. Let N_H be the number of nodes between a node and its hop edge node at the 0th time step. Label the nodes with IDs: $\{0, 1, \ldots N_H + 1\}$, where the reference node has ID 0, and the hop edge node has ID $N_H + 1$. Therefore, $R \le \sum_{i=0}^{N_H+1} X_i(0) < R + X_{N_H+1}(0)$. A node and its hop edge node remain connected until $\sum_{i=0}^{N_H} X_i(m) \ge R$ at some time step m which is the communication link lifetime.

The sum of $(N_H + 1)$ i.i.d. distance headways, where each headway, X_i, is a birth and death Markov chain as illustrated in Figure 1, is an $(N_H + 1)$ dimensional Markov chain. The complexity of this Markov chain is obvious especially when N_H is not small, since a non-zero transition probability to a non-neighboring state is possible. For tractability, we use an alternative approach as follows.

C. Link disconnection events

In this subsection, we present the set of events that cause the disconnection between a reference node and its hop edge node at a certain time step, m. Consider a set $\mathbb{X} = \{X_0, X_1, \ldots, X_{N_H}\}$ of $(N_H + 1)$ distance headways (stochastic processes) between the reference node and its hop edge node, where $\mathbb{X} = \{\mathbb{X}(m), m = 0, 1, 2, \ldots\}$. For notation simplicity, let $\mathbb{X}(m) = \{k_0, k_1, \ldots, k_{N_H}\}$ denote $\{X_i(m) = x_{k_i}\}_{i=0}^{N_H}$. Furthermore, let $\{s_0, s_1, \ldots, s_{N_H}\}$ denote the set of state indices of the $(N_H + 1)$ distance headways at the 0th time step, (i.e., $\{X_i(0) = x_{s_i}\}_{i=0}^{N_H}$), where $s_i \in \{0, 1, 2, \ldots, N_R - 1\}$, and $\sum_{i=0}^{N_H} x_{s_i} < R$. Let E_D be the event that the link between a reference node and its hop edge node, separated by N_H nodes, disconnects given $\mathbb{X}(0)$, and let $E_D(m)$ be the event that this disconnection occurs at the mth time step. When the hop edge node and the reference node are adjacent to each other, i.e., $N_H = 0$, a link disconnection occurs when the distance headway X_0 transits to state N_R. Therefore, $E_D(m) \equiv \{X_0(m) = x_{N_R} | s_0\}$ for $N_H = 0$.

When $N_H > 0$, consider first the case when $\alpha = 0$. A link disconnection occurs at time step m if $\left\{\mathbb{X}(m) = \{k_0, k_1, \ldots, k_{N_H}\}, \sum_{i=0}^{N_H} k_i \geq N_R\right\}$. That is, the set $\{k_i\}_{i=0}^{N_H}$ is an integer partition of a positive integer that is greater than or equal to N_R. In number theory and combinatorics, an ordered integer partition of a positive integer n is a sequence of positive integers whose sum equals n. Each member of the sequence is called a *part*. An ordered J-restricted integer partition of an integer n is an integer partition of n into exactly J parts. Let $\mathbb{A}_J(n) = \{a_1(i), a_2(i), \ldots, a_J(i)\}_{i=1}^{L_J(n)}$ be a set of all possible ordered J-restricted integer partitions of n, where $a_j(i)$, $1 \leq j \leq J$ is the jth part of the ith partition $\mathbb{A}_J^i(n)$, and $L_J(n) = \binom{n-1}{J-1}$ is the total number of such partitions, i.e., the size of set $\mathbb{A}_J(n)$ [21]. For example, $A_2(6) = \{\{1, 5\}, \{5, 1\}, \{2, 4\}, \{4, 2\}, \{3, 3\}\}$, where $A_2^1(6) = \{1, 5\}$, $a_1(1) = 1$, $a_2(4) = 2$ and $L_2(6) = \binom{6-1}{2-1} = 5$. Furthermore, let $\mathbb{K}_J(N_H) = \{k_1(v), k_2(v), \ldots, k_J(v)\}_{v=1}^{K_J(N_H)}$ be the set of all J-combinations of the set $\{0, 1, \ldots, N_H\}$, where $k_j(v)$, $1 \leq j \leq J$, is the jth element of the vth combination, and let $K_J(N_H) = \binom{N_H+1}{J}$ be the number of such combinations. We define two random events, $e_1(m), e_2(m)$ at the mth time step as follows:

$$e_1(m) \equiv \bigcup_{k_0=0}^{N_H} \left\{ X_{k_0}(m) = x_{N_{ED}} \Big| s_{k_0} \right\} \tag{13}$$

$$e_2(m) \equiv \bigcup_{J=2}^{N_H+1} \bigcup_{i=1}^{L_J(N_{ED})} \bigcup_{v=1}^{K_J(N_H)} \Big\{ X_{k_1(v)}(m) \geq x_{a_1(i)},$$
$$X_{k_2(v)}(m) \geq x_{a_2(i)}, \ldots, X_{k_J(v)}(m) \geq x_{a_J(i)} \Big|$$
$$s_{k_1(v)}, s_{k_2(v)}, \ldots, s_{k_J(v)} \Big\}. \tag{14}$$

where $N_{ED} = N_R - \lfloor \frac{\alpha N_H}{(R-\alpha)/N_R} \rfloor$ is an integer such that if set $\mathbb{X}$ is in set of states whose indices construct an integer partition of an integer greater than or equal to N_{ED}, the communication link breaks. Note that N_{ED} accounts for the minimum value of the distance headways (i.e., α), and $N_{ED} = N_R$ for $\alpha = 0$. Event $e_1(m)$ occurs when at least one of the distance headways of set $\mathbb{X}$ is in state N_{ED} at the mth time step, resulting in a link disconnection. Note that N_{ED} is the least state index required for a distance headway to reach in order for the link to disconnect. Event $e_2(m)$ occurs when at least J distance headways of set $\mathbb{X}$ are in states that construct a J-restricted integer partition of an integer that is greater or equal to N_{ED} with parts at most

equal to N_R. Note that N_{ED} accounts for the minimum value of the distance headway, i.e., α. That is, event $e_2(m)$ occurs if J distance headways of set $\mathbb{X}$ are in states $\{k_1, k_2, \ldots, k_J\}$ at the mth time step such that $\sum_{i=1}^{J} k_i \geq N_{ED}$ for any $2 \leq J \leq N_H + 1$. An occurrence of event $e_2(m)$ result in a link disconnection at the mth time step, because the sum $N_{ED} + \lfloor \frac{\alpha N_H}{L} \rfloor$ is equal to N_R, which indicates that the sum of the J distances is greater than or equal to R. Consequently, a link disconnection occurs at the mth time step when either $e_1(m)$ or $e_2(m)$ occurs, i.e., $E_D(m) = \{e_1(m) \cup e_2(m)\}$.

D. Probability distribution of the link lifetime

The lifetime or a communication link from a reference node to its hop edge node, separated by N_H nodes, given $\mathbb{X}(0)$, is the first passage time of event $E_D(m)$, denoted by $T(E_D)$. Let $T(e_i)$ be the first passage time for the occurrence of event $e_i(m)$, $i = 1, 2$ (i.e., $T(e_i) = \min\{m | e_i(m)\}$). The communication link lifetime is calculated by $T(E_D) = \min\{T(e_1), T(e_2)\}$. For $N_H = 0$, this simplifies to $T(E_D) = T(e_1) = T_{s_0, N_{ED}}$, with pmf $P_{T(E_D)}(m)$ which can be calculated using the mth derivative of (11) and (12) for $s_0 = 0$ and $s_0 > 0$, respectively.

For $N_H > 0$, the calculation of the pmf of the link lifetime is not straight forward, due to the obvious correlation between $e_1(m)$ and $e_2(m)$. Let $V = \{V' \bigcup V''\}$ be a matrix resulting from the union of two matrices, V' and V'', with the three matrices having N_H+1 columns. Each unique row of V' consists of J elements equal to one of the partitions in $\mathbb{A}_J(N_{ED})$ and $(N_H - J + 1)$ zero elements, $1 \leq J \leq N_H + 1$. The number of rows of V' is equal to $\sum_{J=1}^{N_{ED}} \binom{N_H+1}{N_H-J+1} \binom{N_{ED}-1}{J-1}$. Matrix V'' is constructed similarly with all possible ordered J-restricted partitions of integers $N_{ED}+1, N_{ED}+2, ..., (N_H+1)N_{ED}$, each with the largest part less than or equal to N_{ED}. For example, for $N_H = 1$, $N_R = 3$, $\alpha = 0$ we have

$$V' = \begin{pmatrix} 3 & 0 \\ 0 & 3 \\ 1 & 2 \\ 2 & 1 \end{pmatrix}, \quad \text{and} \quad V'' = \begin{pmatrix} 1 & 3 \\ 3 & 1 \\ 2 & 2 \\ 3 & 2 \\ 2 & 3 \\ 3 & 3 \end{pmatrix}.$$

A link disconnection occurs at the mth time step when the distance headway set $\mathbb{X}$ is in states $\{u_1, u_2, \ldots, u_{N_H+1}\}$ such that $\{u_1, u_2, \ldots, u_{N_H+1}\}$ is a row in V. Let $E_{D,V}(m) \equiv \{\mathbb{X}(m) = V | \mathbb{X}(0)\}$ be a set of events, each corresponding to set $\mathbb{X}$ being in a set of states that construct one of the rows of V at the mth time step, given $\mathbb{X}(0)$. An event in the set $E_{D,V}(m)$, $E_{D,V(v)}(m)$, $1 < v < |V|$, is the event that the set $\mathbb{X}$ is in states that construct the vth row in V at the mth time step, where $|V|$ is the number of rows in V. An occurrence of event $E_{D,V(v)}(m)$ results in a link disconnection at the mth time step. The first passage time of these events is $T(E_{D,V}) = \min\{m | E_{D,V}(m)\}$. The distribution of $T(E_{D,V})$ can be derived to be

$$P_{T(E_{D,V})}(m)$$
$$= \begin{cases} \prod_{i=0}^{N_H} M'_{s_i+1, v_i+1}, & m = 1 \\ \prod_{i=0}^{N_H} M'^m_{s_i+1, v_i+1} - \left[\sum_{n=1}^{m-1} \left\{ \prod_{j=0}^{N_H} M'^n_{v_j+1, v_j+1} \right\}^t \right. \\ \left. \otimes P_{T(E_{D,V})}(m-n) \right], & m > 1 \end{cases}$$
$$\tag{15}$$

where v_i is the ith column of matrix V and $M'^m_{s_i+1, v_i+1}$ is an array with elements equal to the $(v_i + 1)^{\text{th}}$ entries of the $(s_i + 1)^{\text{th}}$ row of the mth power of matrix M', $1 \leq i, j \leq N_{\max}$, $\{\cdot\}^t$

denotes the transpose matrix operation, and the product notations $\prod$ and $\otimes$ correspond to the general and the Hadamard matrix multiplications, respectively. For $m > 1$, the subtracted term in (15) is to guarantee that none of the $E_{D,V}$ events occurs before time step m, i.e., set $\mathbb{X}$ does not reach states with indices that construct a row in V before time step m. Since the communication link disconnects if any of the events in $E_{D,V}$ occurs, the pmf of the link lifetime is given by

$$P_{T(E_D)}(m) = \sum_{v=1}^{|V|} P_{T(E_{D,V(v)})}(m) \qquad (16)$$

where $|V|$ is the number of rows in matrix V and $V(v)$ is the vth row of V.

VI. RESULTS AND DISCUSSION

This section presents numerical results for the analysis of the pdf of the communication link length, $f_H(h)$, and the pmf of the link lifetime, $P_{T(E_D)}(m)$. We consider three traffic flow conditions, uncongested, near-capacity, and congested, each corresponding to a set of parameters listed in Table II. We set $\sigma = \frac{1000}{2D}$ for the mesoscopic distance headway models. The parameters for the microscopic Markov-chain distance headway model are also listed in Table II, where β, p and q follow the VISSIM data fitting results in subsectionIII-B. Without loss of generality, we set $\alpha = 0$, and $X_{\max} = R$. This is sufficient for communication link analysis, as the link breaks if any X_i's reach state N_R. The values of N_H and $\mathbb{X}(0)$, listed in Table II, are first set to their average values. To verify the link lifetime analysis, we compare the analytical link lifetime pmf calculated with (15) and (16) to that calculated from simulated vehicular traffic. A three-lane highway traffic is simulated using the microscopic vehicle traffic simulator VISSIM as described in subsectionIII-B. The choice of simulating a three-lane highway instead of a single-lane highway is to achieve a more realistic vehicle mobility in which a vehicle can overtake other vehicles and accelerate towards its desired speed. The desired speed for all vehicles is normally distributed with mean 100 kilometer per hour and standard deviation of 10 kilometer per hour. The pmf of the lifetime of a link with initial conditions N_H and $\mathbb{X}(0)$, is calculated by counting the number of occurrences of link breakage at m^{th} time step for $m > 0$ and for all links with initial conditions N_H and $\mathbb{X}(0)$. Six 30-minute simulations are obtained for each of the three vehicle densities. The calculation of the link lifetime pmf, $P_{T(E_D)}(m)$, from the VISSIM simulated vehicle traffic data includes the lifetime of the following: 1) a link between a reference vehicle and its corresponding hop edge node on the same lane, independently of changing hop edge node during the link's lifetime as long as the initial hop edge node remains in the link; and 2) a new link between a reference vehicle and its new hop edge node on the same lane when its previous link breaks. A link which involves a lane change during its lifetime is excluded from the pmf calculation. The frequency of a link lifetime at value l is upper bounded by $\frac{T_{sim}N_S}{l}$, where T_{sim} is the simulation time and N_S is the total number of vehicles in the simulation. The frequency of l-valued lifetime occurrences in

Table II. System parameters in simulation and analysis

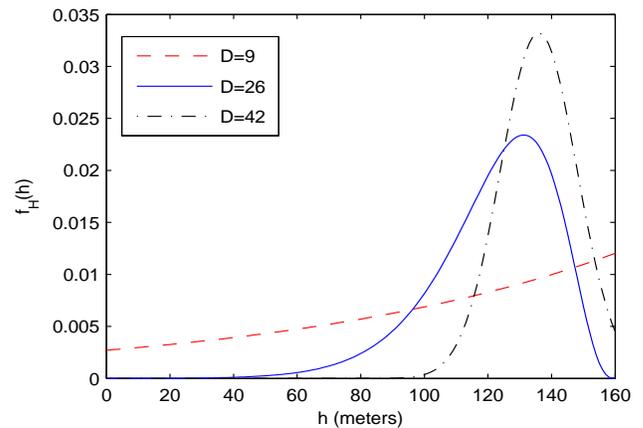| Traffic flow condition	D(veh/km)	N_H	β	p, q	$\mathbb{X}(0)$
Uncongested	9	0	0.4	0.17	{5}
Near-capacity	26	3	0.74	0.23	{1,1,1,1}
Congested	42	5	0.94	0.35	{1,1,1,1,1,1}
R (meter)	N_R	$N_{\max}$	α	τ (second)	**L**(meter)
160	8	9	0	2	20

Figure 7. The probability density function of the hop length for three traffic flow conditions with vehicle densities of 9, 26, and 42 veh/km.

VISSIM data is normalized accordingly in the link lifetime pmf calculation.

Figure 7 plots the pdfs (8)-(10) of the hop length for three vehicle densities $D = 9, 26$, and 42 veh/km with average hop length equal to $99.2, 121.8$, and 132.2 meters, respectively. The average length of the communication link is larger for a higher vehicle density, due to a larger average number of nodes between a node and its hop edge node. Using (1)-(3), the probability for an unavailable link between two vehicles (i.e., $P(X_i > R)$) is $0.23, 5.2 \times 10^{-5}$, and 0 for $D = 9, 26$, and 42 veh/km, respectively. That is, the probability of network fragmentations is higher in an uncongested traffic flow condition than that in a congested traffic flow condition.

Figure 8 plots the pmf of the communication link lifetime for the three traffic flow conditions. The theoretical results are obtained using (12) for the uncongested traffic flow condition and (16) for the near-capacity and congested traffic flow conditions. We use MAPLE to calculate the mth derivative for the generating function in (12). For large values of j and/or j' in (12), we use the mth derivative of the product rule proposed in [22]. The simulation results are calculated from the generated VISSIM vehicle trajectory data. The simulation results closely agree with the theoretical calculations. However, there exist slight differences between simulation and theoretical results. This is mainly due to lane changes, which are not explicitly accounted for in our model. The effect of lane changes is more notable in the low vehicle density simulation results, where we get zero probability for some large link lifetime values, as shown in Figure 8(a). This is due to the high probability of lane change for large link lifetimes, which is excluded from our calculations. The average link lifetime is found to be $335.5, 88.1$, and 65.9 seconds for the low, intermediate, and high vehicle densities, respectively. Recall from subsectionV-C, that the link disconnection event, E_D, depends on the initial conditions N_H and $\mathbb{X}(0)$. In order to extend the results for different initial conditions, we conduct the following: 1) discretize the mesoscopic distance headway models in (1)-(3); 2) using the discretized mesoscopic distance headway models, calculate the probability, $P\left(\mathbb{X}(0) = \{s_i\}_{i=1}^{n} | N_H = n\right)$, that set $\mathbb{X}(0)$ of size n is equal to set $\{s_i\}_{i=1}^{n}$, for $0 \leq s_i \leq N_{\max}$; and 3) using renewal theory, the pmf of the N_H is calculated for each of the mesoscopic distance headway models in (1)-(3) [23]. Therefore, we extend the results for different initial conditions (i.e., N_H and $\mathbb{X}(0)$) for the range of values within which N_H lies with probabilities of 0.94, 0.95, and 0.94 and X lies with probabilities 0.94, 0.97, and 0.99, for $D = 9, 26$, and
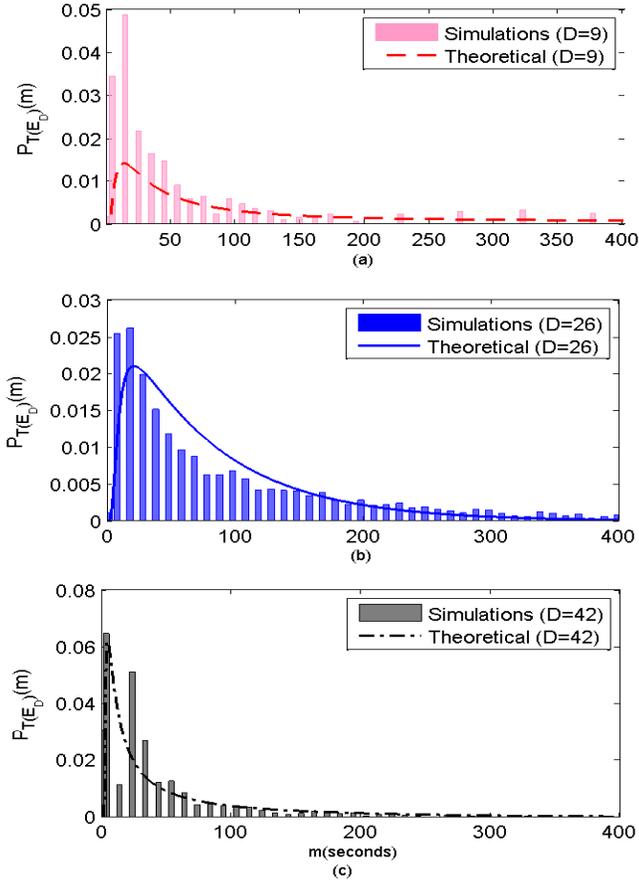
Figure 8. Probability mass function of the communication link lifetime for D = (a) 9, (b) 26, and (c) 42 veh/km.

42 veh/km, respectively. Finally, the low of total probability is used to find the pmf of the link lifetime over the considered set of initial conditions. The average link lifetime, over the considered range of initial conditions, is found to be 145.50, 46.07, and 44.76 seconds for the low, intermediate, and high vehicle density, respectively. Although, intuitively, it is thought that a communication link lasts longer with a higher vehicle density, our results indicate the opposite. The reasons are: 1) the impact of a larger number of vehicles within the link, N_H, with a higher vehicle density and therefore multiple mobility factors on the communication link lifetime; and 2) vehicles tendency to move with their maximum desired speed in an uncongested traffic flow conditions. Since the communication link disconnects when the sum of any $J \leq N_H + 1$ distance headways is greater than R, the larger the N_H value, the more frequently a link breakage occurs, for the same distance headway model. Although distance headways are large in a low vehicle density scenario with free driving (Table I), this does not necessarily indicate a large probability of changing speeds (i.e., large p and q). On the contrary, vehicles are more likely to be at their maximum desired speeds, resulting in small p and q values [5]. In a congested traffic flow condition, vehicles are more likely to undergo stop-and-go situations, in which drivers speed up whenever they get an opportunity (i.e., large p and q values). This agrees with VISSIM results shown in Figure 4.

From the results shown in Figure 7 and Figure 8, we conclude the following: For a high traffic density, there is a higher probability of link availability between two nodes (Figure 7); however, the link lifetime is shorter (Figure 8). This causes the communication link to fluctuate between connection and disconnection more

frequently when compared to that in a low vehicle density. This is due to the stop-and-go scenario in a high vehicle density. On the other hand, for a low traffic density, there is a lower probability of link availability between two nodes (Figure 7); however, if a link exists, the link lasts longer when compared to the case in a high vehicle density (Figure 8). Therefore, when a communication link disconnects in an uncongested traffic flow condition, it has a smaller probability to re-connect than that in a congested traffic flow condition.

It should be noted that our communication link analysis depends only on the link distance. In reality, the communication link between two nodes depends not only on the distance between the two nodes, but also on the communication channel condition. Although the distance between two nodes may be less than the communication range, poor channel conditions may result in inability of the two nodes to communicate. Both vehicle mobility and vehicle density impact the communication channel conditions [24]. Additionally, as the vehicle density increases to a traffic jam situation, the network data load increases. In this case, the communication between two nodes (and, therefore, the link lifetime) is controlled by the network data traffic congestion rather than by vehicle mobility [25]. Extending our communication link analysis to account for the communication channel condition and the network data load needs further investigation.

VII. CONCLUSION

This paper presents a stochastic analysis of the communication link in a highway VANET with focus on a single lane. Mesoscopic mobility models are used to derive the stationary probability density of the communication link length for three traffic flow conditions. A stochastic microscopic model is proposed for the distance headway. The model captures time variations of the distance headway based on a discrete-time Markov chain that preserves the realistic dependency of distance headway changes at consecutive time steps. This dependency increases with the vehicle density, which is consistent with highway data patterns from empirical NGSIM and simulated VISSIM data sets. Further, the distance headway model is used to analyze the communication link lifetime. The first passage time analysis is employed to derive the probability distribution of the communication link lifetime. Numerical results indicate that the communication hop length increases and the link lifetime decreases with an increase in vehicle density. The link length and lifetime statistics are essential to the development of network protocols and algorithms to ensure reliable information delivery in VANETs.

APPENDIX A
HOP LENGTH DISTRIBUTION FOR INTERMEDIATE VEHICLE DENSITY

From (3), the pdf of the inter-vehicle spacing $X \sim Pears(\lambda, z, \alpha)$, and the corresponding cdf is

$$\begin{aligned} F_X(x) &= \int_\alpha^x f_X(x)dx \\ &= \int_\alpha^x (x-\alpha)^{z-1}e^{-\lambda(x-\alpha)}dx. \end{aligned}$$

Letting $u = \lambda(x-\alpha)$,

$$\begin{aligned} F_X(x) &= \frac{\lambda^z}{\Gamma(z)}\int_0^{\frac{x-\alpha}{\lambda}}\left(\frac{u}{\lambda}\right)^{z-1}e^{-u}\lambda du \\ &= \frac{1}{\Gamma(z)}\int_0^{\lambda(x-\alpha)}u^{z-1}e^{-u}du \\ &= \frac{\gamma(z,\lambda(x-\alpha))}{\Gamma(z)}. \end{aligned}$$

From (7), we have

$$F_H(h) = \frac{P\left(A^c(R-h)\right)\left(1 - P(A^c(h))\right)}{1 - P\left(A^c(R)\right)}$$
$$= \frac{(1 - F_X(R-h))F_X(h)}{F_X(R)}.$$

Substituting (17),

$$F_H(h) = \frac{\left[1 - \frac{\gamma(z,\lambda(R-h-\alpha))}{\Gamma(z)}\right]\left[\frac{\gamma(z,\lambda(h-\alpha))}{\Gamma(z)}\right]}{\frac{\gamma(z,\lambda(R-\alpha))}{\Gamma(z)}}$$
$$= \frac{\left[1 - \frac{\gamma(z,\lambda(R-h-\alpha))}{\Gamma(z)}\right]\gamma(z,\lambda(h-\alpha))}{\gamma(z,\lambda(R-\alpha))}.$$

Therefore, $\frac{d}{dh}\frac{\gamma(z,f(h))}{\Gamma(z)} = \frac{f^{z-1}(h)e^{-f(h)}}{\Gamma(z)}\frac{d}{dh}f(h)$. The corresponding pdf $f_H(h) = \frac{d}{dh}F_H(h)$, which leads to

$$f_H(h) = \frac{1}{\gamma(z,\lambda(R-\alpha))}[f_X(R-h)\gamma(z,\lambda(h-\alpha)) + f_X(h)\Gamma(z,\lambda(R-h-\alpha))], \quad \alpha \le h < R - \alpha.$$

ACKNOWLEDGMENT

REFERENCES

[1] K. Abboud and W. Zhuang, "Analysis of communication link lifetime using stochastic microscopic vehicular mobility model," in *Proc. IEEE Globecom*, Atlanta, USA, Dec., 2013.

[2] H. T. Cheng, H. Shan, and W. Zhuang, "Infotainment and road safety service support in vehicular networking: From a communication perspective," *Mechanical Systems and Signal Processing*, vol. 25, no. 6, pp. 2020–2038, 2011.

[3] W. Alasmary and W. Zhuang, "Mobility impact in IEEE802.11p infrastructureless vehicular networks," *Ad Hoc Networks*, vol. 10, no. 2, pp. 222–230, 2012.

[4] D. Kumar, A. A. Kherani, and E. Altman, "Route lifetime based optimal hop selection in VANETs on highway: an analytical viewpoint," *Networking Technologies, Services, and Protocols, Performance of Computer and Communication Networks, Mobile and Wireless Communications Systems*, pp. 799–814, 2006.

[5] A. May, *Traffic Flow Fundamentals*. Prentice Hall, 1990.

[6] M. Krbalek and K. Kittanova, "Theoretical predictions for vehicular headways and their clusters," *Physics: Data Analysis, Statistics and Probability (arXiv)*, 2012.

[7] L. Li, W. Fa, J. Rui, H. Jian-Ming, and J. Yan, "A new car-following model yielding log-normal type headways distributions," *Chinese Physics B*, vol. 19, no. 2, 2010.

[8] G. Yan and S. Olariu, "A probabilistic analysis of link duration in vehicular ad hoc networks," *IEEE Trans. Intelligent Transportation Systems*, vol. 12, no. 4, pp. 1227–1236, 2011.

[9] L. C. Edie and R. S. Foote, "Traffic flow in tunnels," in *Highway Research Board Proceedings*, 1958.

[10] P. Izadpanah, "Freeway travel time prediction using data from mobile probes," Ph.D. dissertation, University of Waterloo, 2010.

[11] F. Hall, "Traffic stream characteristics," *Traffic Flow Theory. US Federal Highway Administration*, 1996.

[12] X. Chen, L. Li, and Y. Zhang, "A markov model for headway/spacing distribution of road traffic," *IEEE Trans. Intelligent Transportation Systems*, vol. 11, no. 4, pp. 773–785, 2010.

[13] Q. Gong, S. Midlam-Mohler, V. Marano, and G. Rizzoni, "An iterative markov chain approach for generating vehicle driving cycles," *SAE Inter. J. Engines*, vol. 4, no. 1, pp. 1035–1045, 2011.

[14] Next generation simulation community, vehicle trajectory data sets. http://ngsim-community.org/. Accessed Nov. 4, 2012.

[15] M. Fellendorf and P. Vortisch, "Microscopic traffic flow simulator VISSIM," *Fundamentals of Traffic Simulation*, pp. 63–93, 2010.

[16] PTV, "VISSIM 5.40 user manual," *Karlsruhe, Germany*, 2012.

[17] T. Hou and V. Li, "Transmission range control in multi-hop packet radio networks," *IEEE Trans. Communications*, vol. 34, no. 1, pp. 38–44, 1986.

[18] Y. Cheng and T. Robertazzi, "Critical connectivity phenomena in multihop radio models," *IEEE Trans. Communications*, vol. 37, no. 7, pp. 770–777, 1989.

[19] J. Fill, "The passage time distribution for a birth-and-death chain: Strong stationary duality gives a first stochastic proof," *J. Theoretical Probability*, vol. 22, no. 3, pp. 543–557, 2009.

[20] Maple, *Maple (Version 13). Waterloo, Ontario, Canada: Waterloo Maple Software*, 2009.

[21] The math forum, "Proof of ordered partioning of integers". http://mathforum.org/. Accessed May 13, 2013.

[22] D. Mazkewitsch, "The n-th derivative of a product," *The American Mathematical Monthly*, vol. 70, no. 7, pp. 739–742, 1963.

[23] D. Cox, *Renewal theory*. Methuen London, 1962.

[24] X. Cheng, C.-X. Wang, D. I. Laurenson, S. Salous, and A. V. Vasilakos, "An adaptive geometry-based stochastic model for non-isotropic MIMO mobile-to-mobile channels," *IEEE Trans. Wireless Communications*, vol. 8, no. 9, pp. 4824–4835, 2009.

[25] S. Öztürk, J. Mišić, and V. B. Mišić, "Reaching spatial or networking saturation in VANET," *EURASIP J. Wireless Communications and Networking*, no. 1, pp. 1–12, 2011.

Khadige Abboud (S'13) received the B.Sc degree in electrical engineering from Kuwait University in 2007. She completed the M.Sc degree in the field of wireless communications at the Department of Electrical and Computer Engineering, University of Waterloo, Canada in 2009. Since 2010, she has been working toward a Ph.D degree at the Department of Electrical and Computer Engineering, University of Waterloo, Canada. Her research interests include communication link analysis, routing, and node cluster stability in vehicular ad hoc networks.

Weihua Zhuang (M93-SM01-F08) has been with the Department of Electrical and Computer Engineering, University of Waterloo, Canada, since 1993, where she is a Professor and a Tier I Canada Research Chair in Wireless Communication Networks. Her current research focuses on resource allocation and QoS provisioning in wireless networks. She is a co-recipient of the Best Paper Awards from the IEEE Globecom 2012 and 2013, the IEEE Multimedia Communications Technical Committee in 2011, IEEE Vehicular Technology Conference (VTC) Fall 2010, IEEE Wireless Communications and Networking Conference (WCNC) 2007 and 2010, IEEE International Conference on Communications (ICC) 2007 and 2012, and the International Conference on Heterogeneous Networking for Quality, Reliability, Security and Robustness (QShine) 2007 and 2008. She received the Outstanding Performance Award 4 times since 2005 from the University of Waterloo, and the Premiers Research Excellence Award in 2001 from the Ontario Government. Dr. Zhuang was the Editor-in-Chief of IEEE Transactions on Vehicular Technology, and the Technical Program Symposia Chair of the IEEE Globecom 2011. She is a Fellow of the IEEE, a Fellow of the Canadian Academy of Engineering (CAE), a Fellow of the Engineering Institute of Canada (EIC), and an elected member in the Board of Governors of the IEEE Vehicular Technology Society. She was an IEEE Communications Society Distinguished Lecturer (2008-2011).